

Three-body decays of sleptons in models with non-universal Higgs masses

Sabine Kraml

*Laboratoire de Physique Subatomique et de Cosmologie, UJF, CNRS/IN2P3, INPG,
53 Avenue des Martyrs, F-38026 Grenoble, France
E-mail: sabine.kraml@cern.ch*

Dao Thi Nhung

*Institute of Physics and Electronics,
10 Dao Tan, Ba Dinh, Hanoi, Vietnam, and
ICTP,
Strada Costiera 11, I-34014 Trieste, Italy
E-mail: tdao0@ictp.it*

ABSTRACT: We compute the three-body decays of charged sleptons and sneutrinos into other sleptons. These decays are of particular interest in SUSY-breaking models with non-universal Higgs mass parameters, where the left-chiral sleptons can be lighter than the right-chiral ones, and lighter than the lightest neutralino. We present the formulas for the three-body decay widths together with a numerical analysis in the context of gaugino-mediated SUSY breaking with a gravitino LSP.

KEYWORDS: Supersymmetry Phenomenology, Supersymmetric Standard Model, Weak Decays.

Contents

1. Introduction	1
2. Three-body decay widths	2
2.1 Generic expressions	2
2.2 Selectron and smuon decays	3
2.3 Sneutrino decays	6
2.4 Stau decays	8
3. Numerical analysis	10
4. Conclusions	16

1. Introduction

If supersymmetry (SUSY) exists at or around the TeV energy scale, experiments at the LHC have excellent prospects to discover it [1, 2]. The discovery of SUSY particles will be followed by detailed measurements [3, 4] of their masses and decay properties, with the aim to eventually determine the underlying high-scale structure of the theory [5–8]. This programme will most likely require that LHC measurements be complemented by precision measurements at an e^+e^- linear collider (ILC and/or CLIC) [9, 10].

Phenomenological studies and experimental simulations to assess the LHC (ILC, CLIC) potential are often done within minimal models of SUSY breaking, thus reducing the number of free parameters from more than a hundred to just a few. In fact, most studies are done within the framework of the so-called ‘constrained MSSM’, CMSSM (often also called minimal supergravity, mSUGRA), which assumes that gaugino masses $m_{1/2}$, scalar masses m_0 , and trilinear couplings A_0 are each unified at the GUT scale. Even if the analysis method applied is in principle model independent, the high-scale model leaves its imprint in, for instance, a particular mass pattern —and thus in the resulting signatures. It is hence important to assure that one does not miss relevant classes of signatures in benchmark studies. One such class of signatures, which we address in this paper, is three-body decays of sleptons.

In general, in SUSY-breaking models with universal scalar and gaugino masses, the right-chiral charged sleptons, $\tilde{\ell}_R$, are lighter than the left-chiral ones and the sneutrinos, $\tilde{\ell}_L$ and $\tilde{\nu}_\ell$ ($\ell = e, \mu, \tau$). The reason is that the renormalization group evolution of $m_{\tilde{\ell}_R}^2$ is dominated by $U(1)_Y$ D-term contributions, while $m_{\tilde{\ell}_L}^2$ receives $SU(2)_L$ and $U(1)_Y$ D-term corrections. This picture changes, however, for non-universal SUSY breaking parameters

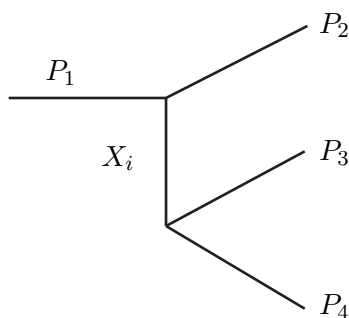


Figure 1: Schematic view of a general three-body decay.

at the high scale, especially for non-universal Higgs-mass parameters $m_{H_{1,2}}^2 \neq m_0^2$, see e.g. [11–13].

Indeed for large enough $m_{H_1}^2 - m_{H_2}^2 > 0$, $\tilde{\ell}_L$ and/or $\tilde{\nu}_\ell$ can become lighter than $\tilde{\ell}_R$, and even lighter than the $\tilde{\chi}_1^0$ [14–16]. In such a setup, if R parity is conserved, the lightest SUSY particle (LSP) should be a gravitino or axino, and the next-to-lightest one (NLSP) a $\tilde{\tau}_1$ or $\tilde{\nu}_\tau$. As observed in [17], SUSY cascade decays are then characterized by three-body decays of left-chiral sleptons at the end of the chain. For example, $\tilde{\chi}_{1,2}^0$ may decay into $\tilde{e}_L e$ (or $\tilde{\tau}_1 \tau$) followed by a three-body decay of the \tilde{e}_L (or $\tilde{\tau}_1$) into a $\tilde{\nu}_\tau$ NLSP. This can considerably influence the collider phenomenology [17].

In this paper, we therefore analyze the three-body decays of $\tilde{\ell}_L$ and $\tilde{\nu}_\ell$ into lighter sleptons, in particular into $\tilde{\tau}_1$ or $\tilde{\nu}_\tau$. To this aim, we have computed all three-body decay widths of sleptons (both left- and right-chiral ones) into other sleptons, and implemented them in SDECAY [18]. Here we give explicit formulas for the relevant decays of $\tilde{\ell}_L$ and $\tilde{\nu}_\ell$ and present a numerical analysis of the branching ratios in the context of gaugino-mediated SUSY breaking. The three-body decays of \tilde{e}_R and $\tilde{\mu}_R$ into $\tilde{\tau}_1$ were discussed in [19, 20] in the context of gauge mediation.

The paper is organized as follows. In section 2 we present the analytic expressions for the decay widths, with the generic structure given in section 2.1 and the particular functions for selectrons/smuons, sneutrinos and staus in sections 2.2–2.4. The numerical analysis is presented in section 3, and section 4 contains our conclusions.

2. Three-body decay widths

2.1 Generic expressions

Consider a general three-body decay of electroweakly interacting particles $P_1 \rightarrow P_2 P_3 P_4$ with masses $m_{1\dots 4}$, momenta $p_{1\dots 4}$, and n_1 exchange particles X_i ($i = 1, \dots, n_1$) as illustrated in figure 1.

The decay width can be written in the form

$$\Gamma_{P_1 \rightarrow P_2 P_3 P_4} = \frac{g^4 m_1}{32(2\pi)^3} \sum_{i,i'=1}^{n_1} \sum_{\alpha=1}^{n_2} c_{ii'}^\alpha I_{ii'}(f^\alpha), \quad (2.1)$$

where g is the SU(2) gauge coupling and we introduce the two-dimensional integral

$$I_{ii'}(f^\alpha) = \int_{2r_2}^{1+r_2^2-(r_3+r_4)^2} dx_2 \int_{x_3^{\min}}^{x_3^{\max}} dx_3 D_{ii'}^X f^\alpha(x_2, x_3). \quad (2.2)$$

Here, the mass ratio $r_j := m_j/m_1$ and integration variable $x_j := 2p_1 p_j/m_1^2$. The integration range (x_3^{\min}, x_3^{\max}) is given by

$$x_3^{\min, \max} = \frac{b \mp \sqrt{\Delta}}{2a}, \quad (2.3)$$

with

$$\begin{aligned} a &= 1 - x_2 + r_2^2, \\ b &= (2 - x_2)(1 - x_2 + r_2^2 + r_3^2 - r_4^2), \\ \Delta &= (x_2^2 - 4r_2^2) [(1 - x_2 + r_2^2 - r_3^2 - r_4^2)^2 - 4r_3^2 r_4^2]. \end{aligned} \quad (2.4)$$

The function $D_{ii'}^X$ is defined as

$$D_{ii'}^X = \Re e \left[\left(a - r_{X_i}^2 - i r_{X_i} \frac{\Gamma_{X_i}}{m_1} \right)^{-1} \left(a - r_{X_{i'}}^2 - i r_{X_{i'}} \frac{\Gamma_{X_{i'}}}{m_1} \right)^{-1} \right], \quad (2.5)$$

with Γ_{X_i} the decay width of the exchange particle X_i . The coefficients c^α and functions f^α can easily be obtained from the squared amplitudes of the contributing diagrams; the sum over $\alpha = 1, \dots, n_2$ has been introduced simply to obtain concise expressions. Below we give the explicit expressions for the processes relevant to our analysis.

2.2 Selectron and smuon decays

Let us start with the decays of selectrons and smuons into $\tilde{\nu}_\tau$ or $\tilde{\tau}_1$. The relevant Feynman diagrams are shown in figure 2. Here and in the following we use the notation $l \equiv e, \mu$. Moreover, $l \equiv l^-, \bar{l} \equiv l^+$, etc. The amplitude for the decay $\tilde{l}_L \rightarrow \tilde{\nu}_\tau \tau \nu_l$, diagram (a) in figure 2, is

$$\begin{aligned} M_{\tilde{l}_L \rightarrow \tilde{\nu}_\tau \tau \nu_l} &= -ig^2 \sum_{j=1}^2 \bar{u}(p_{\nu_l}) (l_j^{\tilde{l}_L} P_R + k_j^{\tilde{l}_L} P_L) \frac{\not{p}_{\nu_l} - \not{p}_{\tilde{l}_L} + m_{\tilde{\chi}_j^\pm}}{m_{\tilde{l}_L}^2 (1 - x_{\nu_l} + r_{\nu_l}^2) - m_{\tilde{\chi}_j^\pm}^2 - i m_{\tilde{\chi}_j^\pm} \Gamma_{\tilde{\chi}_j^\pm}} \\ &\times (l_j^{\tilde{\nu}_\tau} P_R + k_j^{\tilde{\nu}_\tau} P_L) v(p_\tau), \end{aligned} \quad (2.6)$$

where $P_{R,L} = (1 \pm \gamma^5)/2$, and the slepton couplings to charginos are, following [21],

$$\begin{aligned} l_j^{\tilde{l}_L} &= -U_{j1}, & l_j^{\tilde{\nu}_\tau} &= -V_{j1}, \\ k_j^{\tilde{l}_L} &= 0, & k_j^{\tilde{\nu}_\tau} &= h_\tau U_{j2}^*, \end{aligned} \quad (2.7)$$

with U and V the chargino mixing matrices in SLHA [22] notation and $h_\tau = m_\tau/(\sqrt{2}m_W \cos \beta)$ the tau Yukawa coupling. According to eq. (2.1), the decay width can be written as ($m_1 = m_{\tilde{l}_L}$, $n_1 = 2$, $n_2 = 3$)

$$\Gamma_{\tilde{l}_L \rightarrow \tilde{\nu}_\tau \tau \nu_l} = \frac{g^4 m_{\tilde{l}_L}}{32(2\pi)^3} \sum_{j,j'=1}^2 \sum_{\alpha=1}^3 c_{jj'}^\alpha I_{jj'}(f^\alpha), \quad (2.8)$$

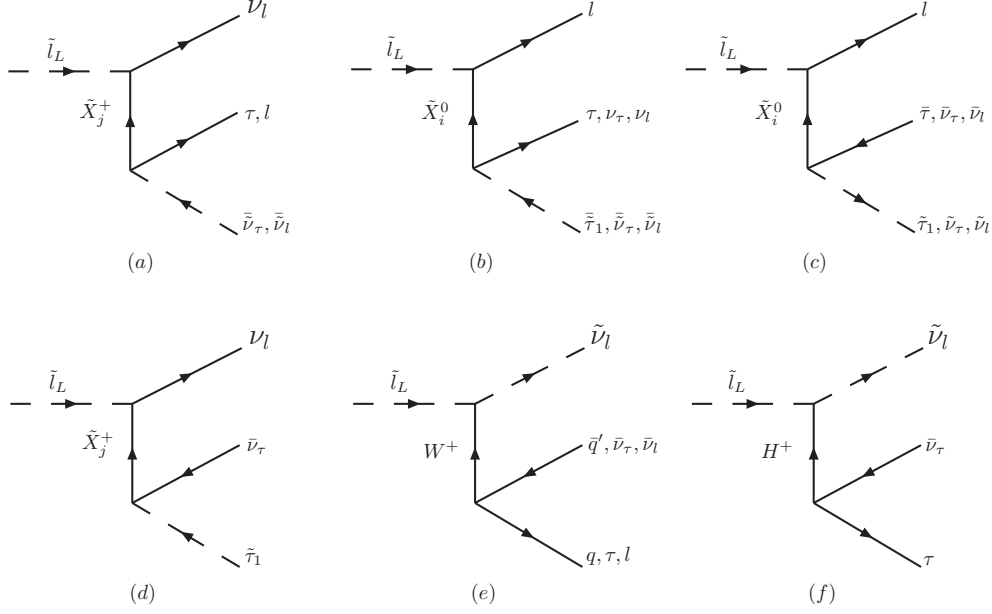


Figure 2: Feynman diagrams for the three-body decays of selectrons and smuons ($i = 1, \dots, 4$; $j = 1, 2$).

with

$$\begin{aligned}
 c_{jj'}^1 &= l_j^{\tilde{\nu}_\tau} l_{j'}^{\tilde{\nu}_\tau*} \tilde{l}_j^{\tilde{L}} \tilde{l}_{j'}^{\tilde{L}*} r_{\tilde{\chi}_j^\pm} r_{\tilde{\chi}_{j'}^\pm}, \\
 c_{jj'}^2 &= k_j^{\tilde{\nu}_\tau} k_{j'}^{\tilde{\nu}_\tau*} \tilde{l}_j^{\tilde{L}} \tilde{l}_{j'}^{\tilde{L}*}, \\
 c_{jj'}^3 &= \tilde{l}_j^{\tilde{L}} \tilde{l}_{j'}^{\tilde{L}*} \Re \left[l_j^{\tilde{\nu}_\tau} k_{j'}^{\tilde{\nu}_\tau*} r_{\tilde{\chi}_j^\pm} + l_{j'}^{\tilde{\nu}_\tau*} k_j^{\tilde{\nu}_\tau} r_{\tilde{\chi}_{j'}^\pm} \right], \\
 f^1 &= -1 + r_{\tilde{\nu}_\tau}^2 - r_\tau^2 + x_\tau + x_{\nu_l}, \\
 f^2 &= 1 - r_{\tilde{\nu}_\tau}^2 + r_\tau^2 - x_\tau - x_{\nu_l} + x_\tau x_{\nu_l}, \\
 f^3 &= r_\tau x_{\nu_l}.
 \end{aligned} \tag{2.9}$$

For the decay $\tilde{l}_L \rightarrow \tilde{\nu}_\tau \nu_\tau l$, figure 2(b), we choose $n_2 = 2$ and obtain

$$\begin{aligned}
 c_{ii'}^1 &= b_i^{\tilde{L}} b_{i'}^{\tilde{L}*} a_i^{\tilde{\nu}_\tau*} a_{i'}^{\tilde{\nu}_\tau}, \\
 c_{ii'}^2 &= a_i^{\tilde{L}} a_{i'}^{\tilde{L}*} a_i^{\tilde{\nu}_\tau*} a_{i'}^{\tilde{\nu}_\tau} r_{\tilde{\chi}_i^0} r_{\tilde{\chi}_{i'}^0}, \\
 f^1 &= 1 - r_{\tilde{\nu}_\tau}^2 - x_l - x_{\nu_\tau} + x_l x_{\nu_\tau}, \\
 f^2 &= -1 + r_{\tilde{\nu}_\tau}^2 + x_l + x_{\nu_\tau}.
 \end{aligned} \tag{2.10}$$

Here the a 's and b 's are the slepton couplings to neutralinos, c.f. [21],

$$\begin{aligned}
 a_i^{\tilde{L}} &= \frac{1}{\sqrt{2}} (\tan \theta_W N_{i1} + N_{i2}), \\
 b_i^{\tilde{L}} &= 0, \\
 a_i^{\tilde{\tau}_1} &= \frac{1}{\sqrt{2}} (\tan \theta_W N_{i1} + N_{i2}) \cos \theta_{\tilde{\tau}} - h_\tau^* N_{i3} \sin \theta_{\tilde{\tau}},
 \end{aligned}$$

$$b_i^{\tilde{\tau}_1} = \sqrt{2} \tan \theta_W N_{i1}^* \sin \theta_{\tilde{\tau}} - h_\tau N_{i3}^* \cos \theta_{\tilde{\tau}}, \quad (2.11)$$

with θ_W the weak mixing angle, $\theta_{\tilde{\tau}}$ the stau mixing angle, and N the neutralino mixing matrix. The decay width for $\tilde{l}_L \rightarrow \tilde{\nu}_\tau \bar{\nu}_\tau l$, figure 2(c), is given by eq. (2.10) with the replacement $a_j^{\tilde{l}_L} \leftrightarrow b_j^{\tilde{l}_L}$.

The decays into $\tilde{\tau}_1$ are also mediated by neutralino and chargino exchange. For the process $\tilde{l}_L \rightarrow \tilde{\tau}_1 \tau l$, figure 2(b), we have $n_1 = 4$, $n_2 = 3$, and

$$\begin{aligned} c_{ii'}^1 &= a_i^{\tilde{l}_L} a_{i'}^{\tilde{l}_L*} b_i^{\tilde{\tau}_1} b_{i'}^{\tilde{\tau}_1*}, \\ c_{ii'}^2 &= a_i^{\tilde{l}_L} a_{i'}^{\tilde{l}_L*} a_i^{\tilde{\tau}_1} a_{i'}^{\tilde{\tau}_1*} r_{\tilde{\chi}_i^0} r_{\tilde{\chi}_{i'}^0}, \\ c_{ii'}^3 &= a_i^{\tilde{l}_L} a_{i'}^{\tilde{l}_L*} \Re \left[a_i^{\tilde{\tau}_1} b_{i'}^{\tilde{\tau}_1*} r_{\tilde{\chi}_i^0} + a_{i'}^{\tilde{\tau}_1*} b_i^{\tilde{\tau}_1} r_{\tilde{\chi}_{i'}^0} \right], \\ f^1 &= 1 - r_{\tilde{\tau}_1}^2 + r_\tau^2 - x_\tau - x_l + x_\tau x_l, \\ f^2 &= -1 + r_{\tilde{\tau}_1}^2 - r_\tau^2 + x_\tau + x_l, \\ f^3 &= r_\tau x_l. \end{aligned} \quad (2.12)$$

The same expressions apply for the process $\tilde{l}_L \rightarrow \tilde{\tau}_1 \bar{\tau} l$, figure 2(c), with $b_i^{\tilde{\tau}_1} \leftrightarrow a_i^{\tilde{\tau}_1}$ in $c_{ii'}^1$ and $c_{ii'}^2$. For the decay through a virtual chargino, $\tilde{l}_L \rightarrow \tilde{\tau}_1 \bar{\nu}_\tau \nu_l$, figure 2(d), we obtain a simple form with $n_1 = 2$, $n_2 = 1$ and

$$\begin{aligned} c_{jj'}^1 &= l_j^{\tilde{\tau}_1} l_{j'}^{\tilde{\tau}_1*} l_j^{\tilde{l}_L} l_{j'}^{\tilde{l}_L*}, \\ f^1 &= 1 - r_{\tilde{\tau}_1}^2 - x_{\nu_l} - x_{\nu_\tau} + x_{\nu_l} x_{\nu_\tau}. \end{aligned} \quad (2.13)$$

We next turn to selectron and smuon decays into sneutrinos of the first two generations. The decay width for $\tilde{e}_L \rightarrow \tilde{\nu}_\mu \mu \nu_e$ ($\tilde{\mu}_L \rightarrow \tilde{\nu}_e \nu_e \mu$), figure 2(a), is in principle given by eq. (2.9) with appropriate replacement of couplings. However, since e and μ masses can be neglected, it simplifies to ($n_1 = 4$, $n_2 = 1$)

$$\begin{aligned} c_{ii'}^1 &= l_j^{\tilde{e}_L} l_{j'}^{\tilde{e}_L*} l_j^{\tilde{\nu}_l} l_{j'}^{\tilde{\nu}_l*} r_{\tilde{\chi}_j^\pm} r_{\tilde{\chi}_{j'}^\pm}, \\ f^1 &= -1 + r_{\tilde{\nu}_\mu}^2 + x_\mu + x_{\nu_e}. \end{aligned} \quad (2.14)$$

For the process $\tilde{e}_L \rightarrow \tilde{\nu}_\mu \nu_\mu e$ ($\tilde{\mu}_L \rightarrow \tilde{\nu}_e \nu_e \mu$), figure 2(b), eq. (2.10) applies with $a_i^{\tilde{\nu}_\tau} \rightarrow a_i^{\tilde{\nu}_l}$. Likewise, the width for $\tilde{e}_L \rightarrow \tilde{\nu}_\mu \bar{\nu}_\mu e$ ($\tilde{\mu}_L \rightarrow \tilde{\nu}_e \bar{\nu}_e \mu$), figure 2(c), is given by eq. (2.10) with $a_i^{\tilde{\nu}_\tau} \rightarrow a_i^{\tilde{\nu}_l}$ and $a_i^{\tilde{l}_L} \leftrightarrow b_i^{\tilde{l}_L}$.

The decay into a sneutrino of the same flavour is more complicated because of interferences between different diagrams. For the decay $\tilde{l}_L \rightarrow \tilde{\nu}_l l \nu_l$, figure 2(a, b) we take the number of exchange particles $n_1 = 6$, with $\tilde{X}_{1\dots 4} = \tilde{\chi}_{1\dots 4}^0$ and $\tilde{X}_{5,6} = \tilde{\chi}_{1,2}^\pm$. Choosing $n_2 = 1$ and indices $i, i' = 1 \dots 4$ for the neutralino exchange and $h, h' = 5, 6$ for the chargino exchange, we obtain

$$\begin{aligned} c_{ii'}^1 &= a_i^{\tilde{l}_L} a_{i'}^{\tilde{l}_L*} a_i^{\tilde{\nu}_l} a_{i'}^{\tilde{\nu}_l*} r_{\tilde{X}_i} r_{\tilde{X}_{i'}}, \\ c_{hh'}^1 &= l_h^{\tilde{\nu}_l} l_{h'}^{\tilde{\nu}_l*} l_h^{\tilde{l}_L} l_{h'}^{\tilde{l}_L*} r_{\tilde{X}_h} r_{\tilde{X}_{h'}}, \\ c_{ih}^1 &= c_{hi}^1 = r_{\tilde{\chi}_i^0} r_{\tilde{X}_h} \Re \left[a_i^{\tilde{l}_L} a_i^{\tilde{\nu}_l} l_h^{\tilde{\nu}_l*} l_h^{\tilde{l}_L*} \right], \end{aligned}$$

$$f^1 = -1 + r_{\tilde{\nu}_l}^2 + x_l + x_{\nu_l}, \quad (2.15)$$

where $\tilde{l}_5^L = \tilde{l}_1^L$, $\tilde{l}_6^L = \tilde{l}_2^L$. We follow the same approach for the decay $\tilde{l}_L \rightarrow \tilde{\nu}_l l \bar{\nu}_l$, which gets contributions from neutralino and W-boson exchange, see figure 2(c, e); $n_1 = 5$ with $\tilde{X}_{1\dots 4} = \tilde{\chi}_{1\dots 4}^0$, $\tilde{X}_5 = W$ and $n_2 = 1$ gives

$$\begin{aligned} c_{ii'}^1 &= a_i^{\tilde{l}_L} a_{i'}^{\tilde{l}_L*} a_i^{\tilde{\nu}_l*} a_{i'}^{\tilde{\nu}_l}, \\ c_{5i}^1 &= c_{i5}^1 = \Re e \left[a_i^{\tilde{l}_L} a_i^{\tilde{\nu}_l*} \right], \\ c_{55}^1 &= 1, \\ f^1 &= 1 - r_{\tilde{\nu}_l}^2 - x_l - x_{\nu_l} + x_l x_{\nu_l}. \end{aligned} \quad (2.16)$$

W-boson exchange also leads to $\tilde{e}_L \rightarrow \tilde{\nu}_e \mu \bar{\nu}_\mu$, $\tilde{\nu}_e \tau \bar{\nu}_\tau$ and $\tilde{\nu}_e q \bar{q}'$, and analogous $\tilde{\mu}_L$ decays. Here we have $n_1 = n_2 = 1$. For $\tilde{e}_L \rightarrow \tilde{\nu}_e \mu \bar{\nu}_\mu$ we obtain

$$\begin{aligned} c_{11}^1 &= 1, \\ f^1 &= 1 - r_{\tilde{\nu}_e}^2 - x_\mu - x_{\nu_\mu} + x_\mu x_{\nu_\mu}, \end{aligned} \quad (2.17)$$

which also applies for the decay into light quarks up to a colour factor 3. Finally, for the decay $\tilde{l}_L \rightarrow \tilde{\nu}_l \tau \bar{\nu}_\tau$ figure 2(e, f) with W and Higgs boson exchanges,

$$\begin{aligned} c_{11}^1 &= 1, \\ c_{22}^2 &= 2 \sin^4 \beta \cos^2 \beta r_W^2 h_\tau^2, \\ c_{12}^2 &= \frac{1}{\sqrt{2}} \sin^2 \beta \cos \beta r_\tau r_W^{-1} h_\tau (r_{\tilde{\nu}_l}^2 - 1), \\ c_{12}^3 &= \frac{1}{\sqrt{2}} \sin^2 \beta \cos \beta r_\tau r_W h_\tau, \\ f^1 &= \frac{1}{4} r_W^{-4} r_\tau^2 (1 - r_{\tilde{\nu}_l}^2)^2 (-1 + r_{\tilde{\nu}_l}^2 - r_\tau^2 + x_\tau + x_{\nu_l}) \\ &\quad + \frac{1}{2} r_W^{-2} r_\tau^2 (1 - r_{\tilde{\nu}_l}^2) (-1 + r_{\tilde{\nu}_l}^2 - r_\tau^2 + x_\tau - x_{\nu_l}) \\ &\quad + \frac{1}{4} r_\tau^2 (3 + r_{\tilde{\nu}_l}^2 - r_\tau^2 + x_\tau - 3x_{\nu_l}) + 1 - r_{\tilde{\nu}_l}^2 - x_\tau - x_{\nu_l} + x_\tau x_{\nu_l}, \\ f^2 &= -1 + r_{\tilde{\nu}_l}^2 - r_\tau^2 + x_\tau + x_{\nu_l}, \\ f^3 &= 1 - r_{\tilde{\nu}_l}^2 + r_\tau^2 + x_\tau - x_{\nu_l}, \end{aligned} \quad (2.18)$$

in which we have used convention $X_1 = W^+$ and $X_2 = H^+$. The remaining coefficients are zero. Analogous expressions of course apply for \tilde{l}_R decays with the appropriate replacements of couplings $\tilde{l}_j^L \rightarrow \tilde{l}_j^R$, etc.

2.3 Sneutrino decays

Since $\tilde{\nu}_{e,\mu}$ are generally lighter than \tilde{e}_L , $\tilde{\mu}_L$, we have to consider but their decays into $\tilde{\nu}_\tau$ or $\tilde{\tau}_1$. The relevant Feynman diagrams are shown in figure 3. For the invisible decays into $\tilde{\nu}_\tau$ plus neutrinos, figure 3(a,b) we find

$$\Gamma_{\tilde{\nu}_l \rightarrow \tilde{\nu}_\tau \bar{\nu}_\tau \nu_l, \tilde{\nu}_\tau \nu_\tau \nu_l} = \frac{g^4 m_{\tilde{\nu}_l}}{32(2\pi)^3} \sum_{i,i'=1}^4 c_{ii'} I_{ii'}(f), \quad (2.19)$$

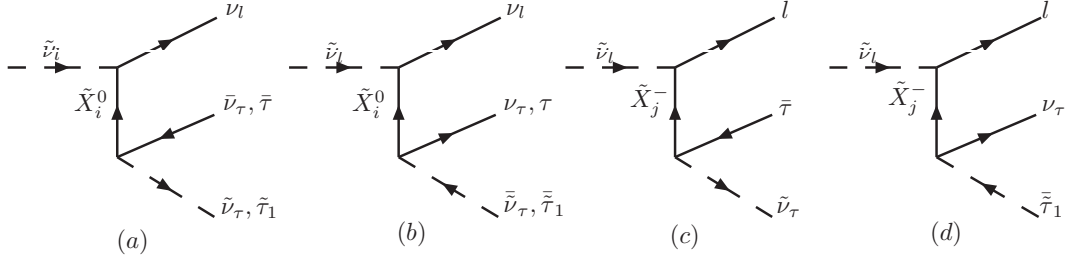


Figure 3: Feynman diagrams for the three-body decays of electron- and muon-sneutrinos ($i = 1, \dots, 4; j = 1, 2$).

in terms of

$$\begin{aligned} c_{ii'} &= a_i^{\tilde{\nu}_l} a_{i'}^{\tilde{\nu}_l*} a_i^{\tilde{\nu}_\tau} a_{i'}^{\tilde{\nu}_\tau*}, \\ f &= 1 - r_{\tilde{\nu}_\tau}^2 - x_{\nu_l} - x_{\nu_\tau} + x_{\nu_l} x_{\nu_\tau} \end{aligned} \quad (2.20)$$

for $\tilde{\nu}_l \rightarrow \tilde{\nu}_\tau \bar{\nu}_\tau \nu_l$ and

$$\begin{aligned} c_{ii'} &= a_i^{\tilde{\nu}_l} a_{i'}^{\tilde{\nu}_l*} a_i^{\tilde{\nu}_\tau} a_{i'}^{\tilde{\nu}_\tau*} r_{\tilde{\chi}_i^0} r_{\tilde{\chi}_{i'}^0}, \\ f &= -1 + r_{\tilde{\nu}_\tau}^2 + x_{\nu_l} + x_{\nu_\tau} \end{aligned} \quad (2.21)$$

for $\tilde{\nu}_l \rightarrow \tilde{\nu}_\tau \nu_\tau \nu_l$. For the decay $\tilde{\nu}_l \rightarrow \tilde{\nu}_\tau \bar{\tau} l$, figure 3(c), we choose $n_2 = 3$, leading to

$$\begin{aligned} c_{jj'}^1 &= l_j^{\tilde{\nu}_l} l_{j'}^{\tilde{\nu}_l*} l_j^{\tilde{\nu}_\tau*} l_{j'}^{\tilde{\nu}_\tau}, \\ c_{jj'}^2 &= l_j^{\tilde{\nu}_l} l_{j'}^{\tilde{\nu}_l*} k_j^{\tilde{\nu}_\tau*} k_{j'}^{\tilde{\nu}_\tau} r_{\tilde{\chi}_j^\pm} r_{\tilde{\chi}_{j'}^\pm}, \\ c_{jj'}^3 &= l_j^{\tilde{\nu}_l} l_{j'}^{\tilde{\nu}_l*} \Re \left[l_j^{\tilde{\nu}_\tau} k_j^{\tilde{\nu}_\tau*} r_{\tilde{\chi}_j^\pm} + l_j^{\tilde{\nu}_\tau*} k_{j'}^{\tilde{\nu}_\tau} r_{\tilde{\chi}_{j'}^\pm} \right], \\ f^1 &= 1 - r_{\tilde{\nu}_\tau}^2 + r_\tau^2 - x_l - x_\tau + x_l x_\tau, \\ f^2 &= -1 + r_{\tilde{\nu}_\tau}^2 - r_\tau^2 + x_l + x_\tau, \\ f^3 &= r_\tau x_l. \end{aligned} \quad (2.22)$$

For the decay $\tilde{\nu}_l \rightarrow \tilde{\tau}_1 \bar{\tau} \nu_l$, figure 3(a), we obtain with $n_2 = 3$:

$$\begin{aligned} c_{ii'}^1 &= a_i^{\tilde{\nu}_l} a_{i'}^{\tilde{\nu}_l*} a_i^{\tilde{\tau}_1*} a_{i'}^{\tilde{\tau}_1}, \\ c_{ii'}^2 &= a_i^{\tilde{\nu}_l} a_{i'}^{\tilde{\nu}_l*} b_i^{\tilde{\tau}_1*} b_{i'}^{\tilde{\tau}_1} r_{\tilde{\chi}_i^0} r_{\tilde{\chi}_{i'}^0}, \\ c_{ii'}^3 &= a_i^{\tilde{\nu}_l} a_{i'}^{\tilde{\nu}_l*} \Re \left[a_i^{\tilde{\tau}_1*} b_{i'}^{\tilde{\tau}_1} r_{\tilde{\chi}_i^0} + a_{i'}^{\tilde{\tau}_1} b_i^{\tilde{\tau}_1*} r_{\tilde{\chi}_{i'}^0} \right], \\ f^1 &= 1 - r_{\tilde{\tau}_1}^2 + r_\tau^2 - x_{\nu_l} - x_\tau + x_{\nu_l} x_\tau, \\ f^2 &= -1 + r_{\tilde{\tau}_1}^2 - r_\tau^2 + x_{\nu_l} + x_\tau, \\ f^3 &= r_\tau x_{\nu_l}. \end{aligned} \quad (2.23)$$

The decay $\tilde{\nu}_l \rightarrow \tilde{\tau}_1 \tau \nu_l$, figure 3(b), is also described by eq. (2.23) with the substitution $a_i^{\tilde{\tau}_1} \leftrightarrow b_i^{\tilde{\tau}_1}$. Finally, for the decay $\tilde{\nu}_l \rightarrow \tilde{\tau}_1 \nu_\tau l$, figure 3(d), we have again a simple form with $n_2 = 1$ and

$$c_{jj'} = l_j^{\tilde{\nu}_l} l_{j'}^{\tilde{\nu}_l*} l_j^{\tilde{\tau}_1} l_{j'}^{\tilde{\tau}_1*} r_{\tilde{\chi}_j^\pm} r_{\tilde{\chi}_{j'}^\pm},$$

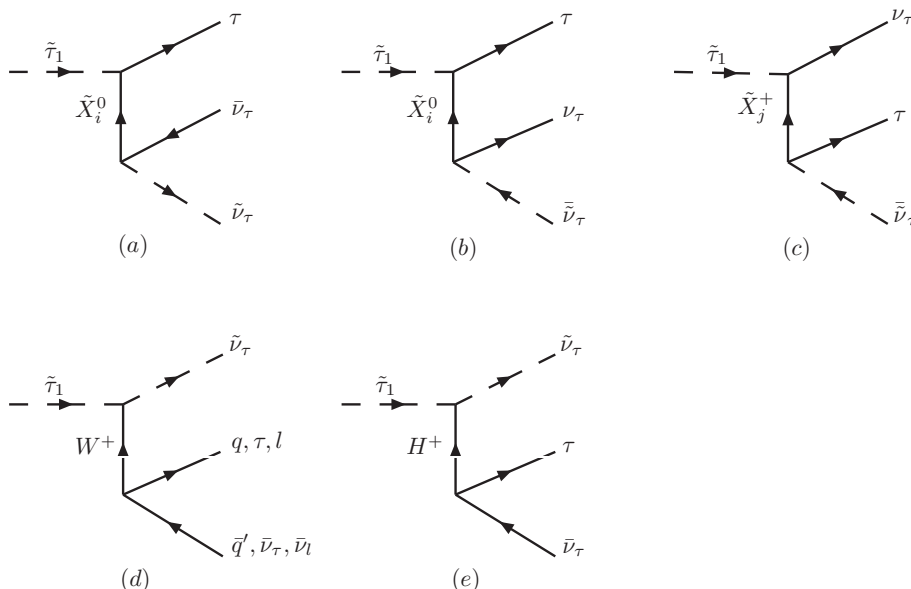


Figure 4: Feynman diagrams for $\tilde{\tau}_1$ decays into $\tilde{\nu}_\tau$.

$$f = -1 + r_{\tilde{\tau}_1}^2 + x_l + x_{\nu_\tau}. \tag{2.24}$$

Last but not least we note that for $\tilde{\nu}_\tau$ decays into $\tilde{\tau}_1$ one has to add the diagram with an off-shell W boson (which is actually the dominant one) and the according interference terms. This is analogous to the $\tilde{\tau}_1$ decays described in the next section.

2.4 Stau decays

The $\tilde{\tau}_1$ typically being lighter than the sleptons of the first and second generation, only stau decays into $\tilde{\nu}_\tau$ are relevant to our analysis. They proceed through exchange of neutralinos, charginos, W or charged Higgs as shown in figure 4.

We start with the easiest process, $\tilde{\tau}_1 \rightarrow \tilde{\nu}_\tau l \bar{\nu}_l$, figure 4(d), for which the decay width is given by

$$\Gamma_{\tilde{\tau}_1 \rightarrow \tilde{\nu}_\tau l \bar{\nu}_l} = \frac{g^4 m_{\tilde{\tau}_1}}{32(2\pi)^3} I(f) \tag{2.25}$$

with

$$f = \cos^2 \theta_\tau (1 - r_{\tilde{\nu}_\tau}^2 - x_l - x_{\nu_l} + x_l x_{\nu_l}). \tag{2.26}$$

This result can be applied for the decay $\tilde{\tau}_1 \rightarrow \tilde{\nu}_\tau q \bar{q}'$ by multiplying with color factor 3. For the decays involving taus in the final state, also the neutralino, chargino, and charged-Higgs exchange contributions have to be taken into account. For the process $\tilde{\tau}_1 \rightarrow \tilde{\nu}_\tau \tau \bar{\nu}_\tau$, figure 4(a, d, e), we take $n_1 = 6$ and $n_2 = 6$, leading to

$$\Gamma_{\tilde{\tau}_1 \rightarrow \tilde{\nu}_\tau \tau \bar{\nu}_\tau} = \frac{g^4 m_{\tilde{\tau}_1}}{32(2\pi)^3} \sum_{\alpha, \alpha'=1}^6 \sum_{\beta=1}^6 c_{\alpha\alpha'}^\beta I_{\alpha\alpha'}(f^\beta), \tag{2.27}$$

with the convention $X_{1\dots 4} = \tilde{\chi}_{1\dots 4}^0$, $X_5 = W^+$ and $X_6 = H^+$. The coefficients and functions in eq. (2.27) are ($i, i' = 1, \dots, 4$)

$$\begin{aligned}
 c_{ii'}^1 &= a_i^{\tilde{\tau}_1} a_{i'}^{\tilde{\tau}_1*} a_i^{\tilde{\nu}_\tau} a_{i'}^{\tilde{\nu}_\tau*}, \\
 c_{ii'}^2 &= b_i^{\tilde{\tau}_1} b_{i'}^{\tilde{\tau}_1*} a_i^{\tilde{\nu}_\tau} a_{i'}^{\tilde{\nu}_\tau*} r_{X_i^0} r_{X_{i'}^0}, \\
 c_{5i}^2 &= c_{i5}^2 = \frac{1}{2} \cos \theta_\tau r_W^{-2} r_\tau r_{\tilde{\chi}_i^0} (1 - r_{\tilde{\nu}_\tau}^2) \Re \left[b_i^{\tilde{\tau}_1} a_i^{\tilde{\nu}_\tau*} \right], \\
 c_{66}^2 &= h_\tau^2 a_{H\tilde{\tau}\tilde{\nu}_\tau}^2 \sin^2 \beta, \\
 c_{ii'}^3 &= r_\tau a_i^{\tilde{\nu}_\tau} a_{i'}^{\tilde{\nu}_\tau*} \Re \left[a_i^{\tilde{\tau}_1} b_{i'}^{\tilde{\tau}_1*} r_{X_{i'}^0} + a_{i'}^{\tilde{\tau}_1*} b_i^{\tilde{\tau}_1} r_{X_i^0} \right], \\
 c_{5i}^3 &= c_{i5}^3 = \frac{1}{2} \cos \theta_\tau r_W^{-2} r_\tau^2 (1 - r_{\tilde{\nu}_\tau}^2) \Re \left[a_i^{\tilde{\tau}_1} a_i^{\tilde{\nu}_\tau*} \right], \\
 c_{5i}^4 &= c_{i5}^4 = \frac{1}{2} \cos \theta_\tau \Re \left[a_i^{\tilde{\tau}_1} a_i^{\tilde{\nu}_\tau*} \right], \\
 c_{5i}^5 &= c_{i5}^5 = \frac{1}{2} \cos \theta_\tau r_{\tilde{\chi}_i^0} r_\tau \Re \left[b_i^{\tilde{\tau}_1} a_i^{\tilde{\nu}_\tau*} \right], \\
 c_{55}^6 &= \cos \theta_\tau^2, \\
 f^1 &= 1 - r_{\tilde{\nu}_\tau}^2 + r_\tau^2 r_{\tilde{\nu}_\tau}^2 - r_\tau^4 - x_\tau - x_{\tilde{\nu}_\tau} - x_{\tilde{\nu}_\tau} r_\tau^2 + x_\tau r_\tau^2 + x_{\tilde{\nu}_\tau} x_\tau, \\
 f^2 &= -1 + r_{\tilde{\nu}_\tau}^2 - r_\tau^2 + x_\tau + x_{\tilde{\nu}_\tau}, \\
 f^3 &= -1 + r_{\tilde{\nu}_\tau}^2 - r_\tau^2 + x_\tau, \\
 f^4 &= 2 - 2r_{\tilde{\nu}_\tau}^2 + r_\tau^2 + r_{\tilde{\nu}_\tau}^2 r_\tau^2 - r_\tau^4 - 2x_{\tilde{\nu}_\tau} - 2x_{\tilde{\nu}_\tau} r_\tau^2 - 2x_\tau + x_\tau r_\tau^2 + 2x_\tau x_{\tilde{\nu}_\tau}, \\
 f^5 &= -1 + r_{\tilde{\nu}_\tau}^2 - r_\tau^2 - x_{\tilde{\nu}_\tau} + x_\tau, \\
 f^6 &= \frac{1}{4} r_W^{-4} r_\tau^2 (1 - r_{\tilde{\nu}_\tau}^2)^2 (-1 + r_{\tilde{\nu}_\tau}^2 - r_\tau^2 + x_\tau + x_{\tilde{\nu}_\tau}) \\
 &\quad + \frac{1}{2} r_W^{-2} r_\tau^2 (1 - r_{\tilde{\nu}_\tau}^2) (-1 + r_{\tilde{\nu}_\tau}^2 - r_\tau^2 + x_\tau - x_{\tilde{\nu}_\tau}) \\
 &\quad + \frac{1}{4} r_\tau^2 (3 + r_{\tilde{\nu}_\tau}^2 - r_\tau^2 + x_\tau - 3x_{\tilde{\nu}_\tau}) + 1 - r_{\tilde{\nu}_\tau}^2 - x_\tau - x_{\tilde{\nu}_\tau} + x_\tau x_{\tilde{\nu}_\tau},
 \end{aligned} \tag{2.28}$$

$$\tag{2.29}$$

with

$$a_{H\tilde{\tau}\tilde{\nu}_\tau} = \frac{1}{\sqrt{2}} (h_\tau^2 - 1) r_W^{-1} \sin 2\beta \cos \theta_\tau + h_\tau \sin \theta_\tau (\sin \beta A_\tau + \cos \beta \mu) / m_{\tilde{\tau}_1}. \tag{2.30}$$

The remaining coefficients are zero. Equation (2.27) also applies to the decay $\tilde{\tau}_1 \rightarrow \tilde{\nu}_\tau \tau \nu_\tau$, figure 4(b, c), with $X_{1\dots 4} = \tilde{\chi}_{1\dots 4}^0$ and $X_{5,6} = \tilde{\chi}_{1,2}^\pm$:

$$\begin{aligned}
 c_{ii'}^1 &= b_i^{\tilde{\tau}_1} b_{i'}^{\tilde{\tau}_1*} a_i^{\tilde{\nu}_\tau} a_{i'}^{\tilde{\nu}_\tau*}, \\
 c_{ii'}^2 &= a_i^{\tilde{\tau}_1} a_{i'}^{\tilde{\tau}_1*} a_i^{\tilde{\nu}_\tau} a_{i'}^{\tilde{\nu}_\tau*} r_{\tilde{\chi}_i^0} r_{\tilde{\chi}_{i'}^0}, \\
 c_{hh'}^2 &= l_h^{\tilde{\nu}_\tau} l_{h'}^{\tilde{\nu}_\tau*} l_h^{\tilde{\tau}_1} l_{h'}^{\tilde{\tau}_1*} r_{\tilde{X}_h} r_{\tilde{X}_{h'}}, \\
 c_{ih}^2 &= c_{hi}^2 = r_{\tilde{\chi}_i^0} r_{\tilde{X}_h} \Re \left[a_i^{\tilde{\tau}_1} a_i^{\tilde{\nu}_\tau} l_h^{\tilde{\nu}_\tau*} l_h^{\tilde{\tau}_1*} \right], \\
 c_{ii'}^3 &= a_i^{\tilde{\nu}_\tau} a_{i'}^{\tilde{\nu}_\tau*} \Re \left[a_i^{\tilde{\tau}_1} b_{i'}^{\tilde{\tau}_1*} r_{\tilde{\chi}_i^0} + b_i^{\tilde{\tau}_1} a_{i'}^{\tilde{\tau}_1*} r_{\tilde{\chi}_{i'}^0} \right], \\
 c_{ih}^3 &= c_{hi}^3 = r_{\tilde{X}_h} \Re \left[b_i^{\tilde{\tau}_1} a_i^{\tilde{\nu}_\tau} l_h^{\tilde{\nu}_\tau*} l_h^{\tilde{\tau}_1*} \right],
 \end{aligned}$$

$$\begin{aligned}
 c_{hh'}^4 &= l_h^{\tilde{\tau}_1} l_{h'}^{\tilde{\tau}_1*} \Re \left[l_h^{\tilde{\nu}_\tau} k_{h'}^{\tilde{\nu}_\tau*} r_{\tilde{X}_h} + k_h^{\tilde{\nu}_\tau} l_{h'}^{\tilde{\nu}_\tau*} r_{\tilde{X}_{h'}} \right], \\
 c_{ih}^4 &= c_{hi}^4 = r_{\tilde{X}_i} \Re \left[a_i^{\tilde{\tau}_1} l_h^{\tilde{\tau}_1*} a_i^{\tilde{\nu}_\tau} k_h^{\tilde{\nu}_\tau*} \right], \\
 c_{hh'}^5 &= k_h^{\tilde{\nu}_\tau} k_{h'}^{\tilde{\nu}_\tau*} l_h^{\tilde{\tau}_1} l_{h'}^{\tilde{\tau}_1*}, \\
 c_{ik}^6 &= c_{ki}^6 = \Re \left[b_i^{\tilde{\tau}_1} a_i^{\tilde{\nu}_\tau} k_h^{\tilde{\nu}_\tau*} l_h^{\tilde{\tau}_1*} \right], \\
 f^1 &= 1 - r_{\tilde{\nu}_\tau}^2 + r_\tau^2 r_{\tilde{\nu}_\tau}^2 - r_\tau^4 - x_{\nu_\tau} r_\tau^2 + x_\tau r_\tau^2 - x_\tau - x_{\nu_\tau} + x_\tau x_{\nu_\tau}, \\
 f^2 &= -1 + r_{\tilde{\nu}_\tau}^2 - r_\tau^2 + x_\tau + x_{\nu_\tau}, \\
 f^3 &= r_\tau (-1 + r_{\tilde{\nu}_\tau}^2 - r_\tau^2 + x_\tau), \\
 f^4 &= r_\tau x_{\nu_\tau}, \\
 f^5 &= 1 - r_{\tilde{\nu}_\tau}^2 + r_\tau^2 - x_\tau - x_{\nu_\tau} + x_\tau x_{\nu_\tau}, \\
 f^6 &= -1 + r_{\tilde{\nu}_\tau}^2 - r_\tau^2 + r_\tau^2 x_{\nu_\tau} + x_\tau + x_{\nu_\tau} - x_\tau x_{\nu_\tau}.
 \end{aligned} \tag{2.31}$$

Here indices $i, i' = 1, \dots, 4$ and $h, h' = 5, 6$, and we have used the same convention for the couplings as in eq. (2.15). The remaining coefficients are zero.

The three-body decays of $\tilde{\nu}_\tau$ into a $\tilde{\tau}_1$ NLSP are simply given by the inverse diagrams of figure 4.

3. Numerical analysis

In order to perform a numerical analysis, we have implemented the slepton three-body decays in SDECAY [18]. The decay widths of virtual SUSY particles (charginos and neutralinos) are taken into account as computed by SDECAY. The width of the charged Higgs boson is taken from HDECAY [23] through the SUSYHIT [24] interface. We have checked our code against CALCHEP [25] and found good agreement.

As mentioned in the Introduction, three-body decays of left-chiral sleptons are of particular interest in models with non-universal Higgs-mass parameters at the high scale. A very attractive realization of such a model is the case of gaugino mediation [26, 27], where supersymmetry breaking occurs on a four-dimensional brane within a higher-dimensional theory. In such a setting, if gauge and Higgs superfields live in the bulk with direct couplings the chiral superfield S responsible for SUSY breaking, while squarks and sleptons are confined to some branes without direct coupling to S , we have the following boundary conditions at the compactification scale M_C [27]:¹

$$\begin{aligned}
 g_1 &= g_2 = g_3 = g \simeq 1/\sqrt{2}, \\
 M_1 &= M_2 = M_3 = m_{1/2}, \\
 m_0^2 &= 0 \quad \text{for all squarks and sleptons,} \\
 A_0 &= 0, \\
 \mu, B\mu, m_{H_{1,2}}^2 &\neq 0,
 \end{aligned} \tag{3.1}$$

with GUT charge normalization used for g_1 . The superparticle spectrum is determined from these boundary conditions and the renormalisation group equations. The free parameters

¹In our notation, $m_{H_1}^2 = m_{H_d}^2$ and $m_{H_2}^2 = m_{H_u}^2$.

of the model are hence $m_{1/2}$, $m_{H_1}^2$, $m_{H_2}^2$, $\tan\beta$, and the sign of μ ; $|\mu|$ being determined by radiative electroweak symmetry breaking.

The parameter ranges leading to a viable low-energy spectrum were discussed in [14, 15] assuming $M_C = M_{\text{GUT}}$. In [16] it was shown that either the lightest neutralino or the gravitino can be viable dark matter candidates in this model. In particular, ref. [16] discussed the possibility of a gravitino LSP with a stau or tau-sneutrino NLSP. The collider phenomenology was discussed in [15] for the case of a neutralino LSP, and in [17] for the case of a gravitino LSP with a sneutrino NLSP. In this latter paper it was noticed that the left-chiral sleptons are often lighter than the $\tilde{\chi}_1^0$ and then have only three-body decays into lighter sleptons (the decay into the gravitino LSP being relevant only for the NLSP).

Extending ref. [17], we here perform a detailed numerical analysis of the three-body slepton decays in gaugino-mediated SUSY breaking. To this aim, we assume that the gravitino is the LSP and concentrate on scenarios with a stau or sneutrino NLSP. Following [14, 16, 17], we take $m_t = 172.5 \text{ GeV}$, $m_b(m_b) = 4.25 \text{ GeV}$ and $\alpha_s^{\text{SM}}(M_Z)^{\overline{\text{MS}}} = 0.1187$ as SM input parameters. Moreover, we assume $M_C = M_{\text{GUT}}$ and use SOFTSUSY 2.0.14 [28] to compute the sparticle and Higgs masses and mixing angles. In order not to vary too many parameters, we focus on $\tan\beta = 10$ and $m_{H_2}^2 = 0$.

Figure 5 shows the regions of neutralino, tau-sneutrino and stau NLSP in gaugino mediation with a gravitino LSP in the $m_{1/2}$ versus $m_{H_1}^2$ plane. The borders where three-body decays of $\tilde{\tau}_1$, $\tilde{l}_L = (\tilde{e}_L, \tilde{\mu}_L)$, and $\tilde{\nu}_l = \tilde{\nu}_{e,\mu}$ set in, are also indicated (three-body decays of $\tilde{\nu}_\tau$ only occur in the stau NLSP region). As can be seen, three-body decays are important not only for $\tilde{\tau}_1$ and $\tilde{\nu}_\tau$, which always have a small mass difference [17], but also for \tilde{e}_L , $\tilde{\mu}_L$ and $\tilde{\nu}_{e,\mu}$. Note also that here the lightest neutralino can have visible decays like, for instance, $\tilde{\chi}_1^0 \rightarrow \tilde{\tau}_1^\pm \tau^\mp$. The relevant sparticle masses are shown explicitly in figure 6. This figure also shows that the third generation sleptons are indeed always lighter than the first and second generation ones.

A comment is in order concerning BBN constraints. Gaugino mediation gives a lower bound [29] on the gravitino mass, which depends on $m_{1/2}$, the number of dimensions and the compactification scale. For $M_C = M_{\text{GUT}}$ and a gluino mass of about 1 TeV, this bound is roughly $m_{3/2} \gtrsim 20$ to 0.1 GeV for 5 to 10 dimensions [29]. Hence both a $\tilde{\nu}_\tau$ as well as a $\tilde{\tau}_1$ NLSP in the $\sim 100 \text{ GeV}$ mass range can be in agreement with BBN. We do not discuss this any further here but refer to [16, 17] for details.

Another comment concerns the overall parameter space of gaugino mediation. While we here concentrate on $\tan\beta = 10$ and $m_{H_2}^2 = 0$, it is interesting to see which values these parameters could take in the general case. To this aim, figure 7 shows results from a random scan over $m_{H_1}^2$, $m_{H_2}^2$ and $\tan\beta$, for $m_{1/2} = 500 \text{ GeV}$. The left panel shows the projection onto the $m_{H_1}^2$ versus $\tan\beta$ plane, and the right panel the projection onto the $m_{H_2}^2$ versus $\tan\beta$ plane. The grey, yellow and orange points feature $\tilde{\chi}_1^0$, $\tilde{\tau}_1$ and $\tilde{\nu}_\tau$ NLSPs, respectively. The green points also have a $\tilde{\tau}_1$ NLSP, however with a mass-ordering $m_{\tilde{\tau}_1} < m_{\tilde{\chi}_1^0} < m_{\tilde{\nu}_\tau}$ for which no three-body decays of sleptons occur (in most of these cases, $\tilde{\tau}_1 \sim \tilde{\tau}_R$). We conclude that, at $m_{1/2} = 500 \text{ GeV}$, three-body slepton decays occur in the range $m_{H_1}^2 \simeq 1.3\text{--}4.1 \text{ TeV}^2$, $m_{H_2}^2 \lesssim 0.6 \text{ TeV}^2$ and $\tan\beta \simeq 5\text{--}27$. Our choice of

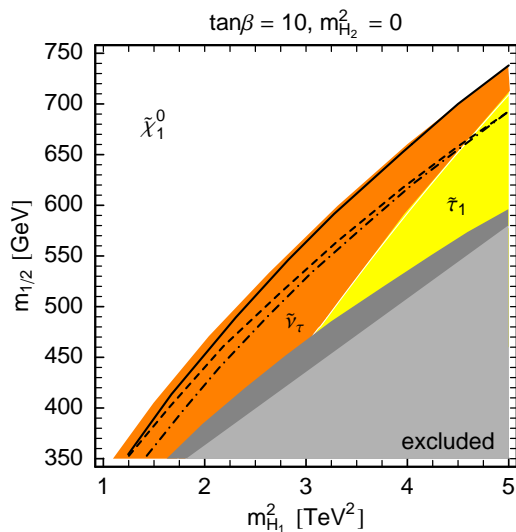


Figure 5: Regions of neutralino (white), sneutrino (orange) and stau (yellow) NLSP in gaugino mediation with a gravitino LSP. Below the full, dashed and dash-dotted lines, respectively, $\tilde{\tau}_1$, \tilde{l}_L and $\tilde{\nu}_l$ have only three-body decays. The grey regions are excluded, either because no viable spectrum is obtained (light grey), or because $m_{\tilde{\tau}_1} < 90$ GeV (medium grey).

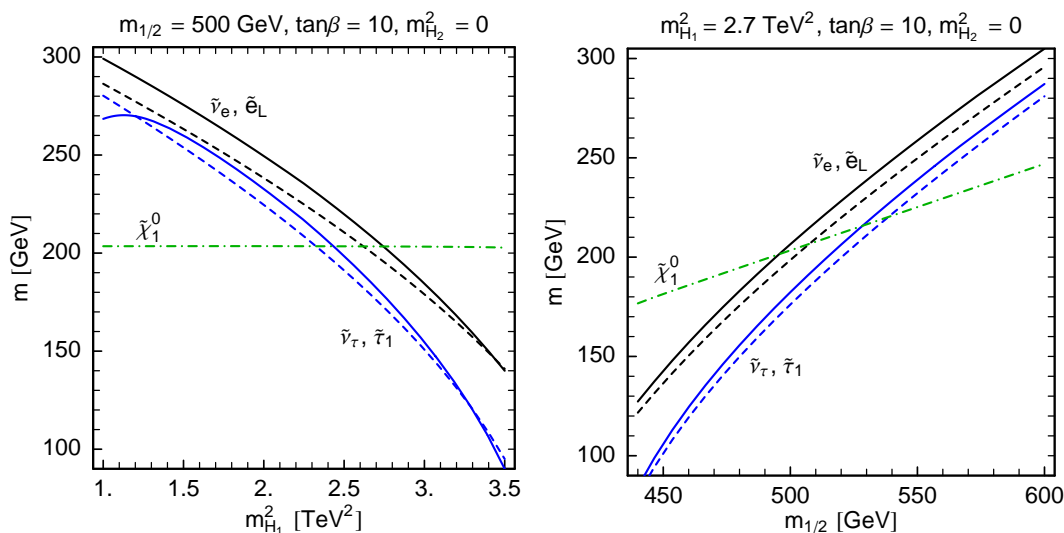


Figure 6: Slepton and neutralino masses as function of $m_{H_1}^2$ (left) and $m_{1/2}$ (right). The dash-dotted green line is for $\tilde{\chi}_1^0$, the full and dashed blue lines are for $\tilde{\tau}_1$ and $\tilde{\nu}_\tau$, and the full and dashed black lines are for \tilde{e}_L and $\tilde{\nu}_e$.

$\tan \beta = 10$ is hence arbitrary, while the choice of $m_{H_2}^2 = 0$ is justified by the fact that the key parameter is $m_{H_1}^2 - m_{H_2}^2$. Indeed, the yellow and orange points in figure 7 all lie within $m_{H_1}^2 - m_{H_2}^2 \simeq 1.2 - 3.7 \text{ TeV}^2$.

Let us now turn to the slepton branching ratios. The branching ratios for \tilde{e}_L decays are shown in figure 8 as function of $m_{H_1}^2$ for $m_{1/2} = 450, 500, 550$ and 600 GeV. The border between tau-sneutrino and stau NLSP is indicated as a thin vertical line. In the

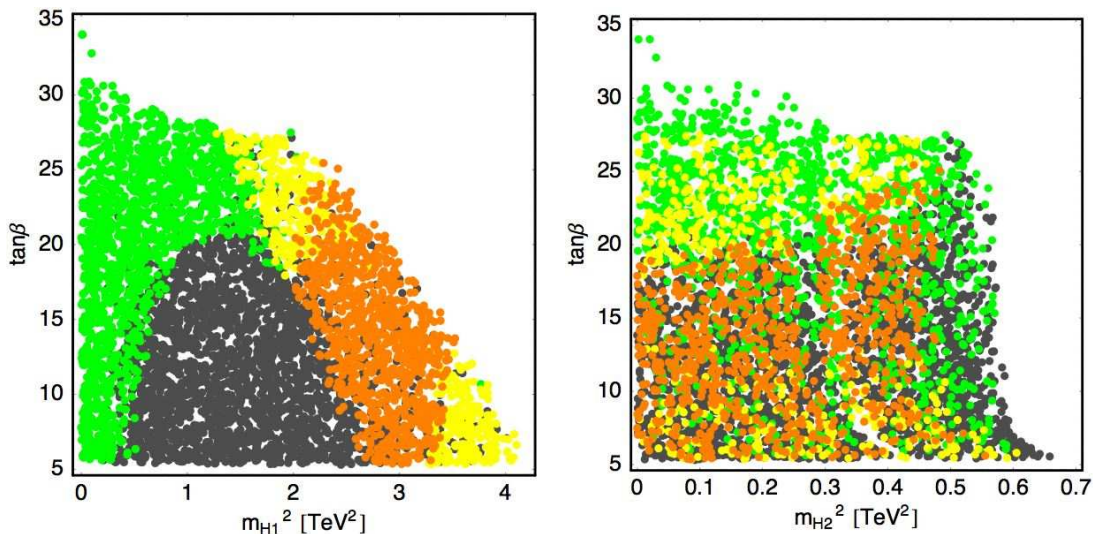


Figure 7: The parameter space of gaugino mediation for $m_{1/2} = 500$ GeV from a random scan over $m_{H_1}^2$, $m_{H_2}^2$ and $\tan\beta$, in the left panel marginalized over $m_{H_2}^2$ and in the right panel marginalized over $m_{H_1}^2$. Parameter points with a $\tilde{\chi}_1^0$, $\tilde{\tau}_1$ and $\tilde{\nu}_\tau$ NLSP are shown in grey, green/yellow or orange, respectively. Three-body slepton decays occur for the yellow and orange points.

plot with $m_{1/2} = 450$ GeV, the NLSP is always the $\tilde{\nu}_\tau$, and decays into it clearly dominate. It is interesting to note, however, that with increasing $m_{H_1}^2$, i.e. increasing mass differences between \tilde{e}_L and $\tilde{\nu}_\tau$ as well as between $\tilde{\chi}_1^0$ and \tilde{e}_L , the decay into $\tilde{\nu}_\tau\nu_e\tau^-$ (mediated by chargino exchange) becomes more important than that into $\tilde{\nu}_\tau\tilde{\nu}_\tau e^-$ (mediated by neutralino exchange).² If the \tilde{e}_L originates from a neutralino decay, $\tilde{\chi}_i^0 \rightarrow \tilde{e}_L^\pm e^\mp$, the former leads to a $\tau^\pm e^\mp E_T^{\text{miss}}$ signature, which could mimic flavour violation. Another interesting observation is that, although the $\tilde{\nu}_\tau$ is lighter than the $\tilde{\tau}_1$, \tilde{e}_L decays into $\tilde{\tau}_1$ amount to 30–40%. Here note also the asymmetry between the $\tilde{\tau}_1^+\tau^-e^-$ and $\tilde{\tau}_1^-\tau^+e^-$ final states. Again we have mixed-flavour final states.

For higher values of $m_{1/2}$, there are also $\tilde{\tau}_1$ NLSP regions; they become larger with increasing $m_{1/2}$. Consequently, the \tilde{e}_L decays into $\tilde{\tau}_1$ get to dominate over those into $\tilde{\nu}_\tau$, c.f. the plots for $m_{1/2} = 500$ –600 GeV in figure 8. The \tilde{e}_L -NLSP mass differences range from 30–50 (60) GeV for $m_{1/2} = 450$ (600) GeV, and the total decay widths are about 10^{-8} – 10^{-6} GeV. Last but not least note that the decays into $\tilde{\nu}_e$, as well as decays into $\tilde{\tau}_1$ plus neutrinos, are negligible throughout the parameter space considered here.

We next discuss the $\tilde{\nu}_e$ decays, for which the branching ratios are shown in figure 9. On the one hand, decays into tau-sneutrino plus neutrinos, $\tilde{\nu}_e \rightarrow \tilde{\nu}_\tau\nu_\tau\nu_e$ (where the bars indicating anti-(s)neutrinos have been omitted for simplicity), clearly dominate for a $\tilde{\nu}_\tau$ NLSP, in which case they are invisible. On the other hand, $\tilde{\nu}_e$ decays into $\tilde{\tau}_1$ can give a visible sneutrino signature. The decay into $\tilde{\tau}_1^\pm\tau^\mp\nu_e$ can be relevant in the $\tilde{\nu}_\tau$ NLSP region for

²The reason is that at $m_{H_1}^2 \simeq 2.26$ TeV², where the three-body decays set in, the $\tilde{\chi}_1^0$ is only slightly heavier than the \tilde{e}_L and thus the mass ratio $r_{\tilde{\chi}_1^0} = m_{\tilde{\chi}_1^0}/m_{\tilde{e}_L} \sim 1$ in eq. (2.5), corresponding to a resonance point. For increasing $m_{H_1}^2$, the \tilde{e}_L becomes lighter, $r_{\tilde{\chi}_1^0}$ increases, and the neutralino exchange becomes less important.

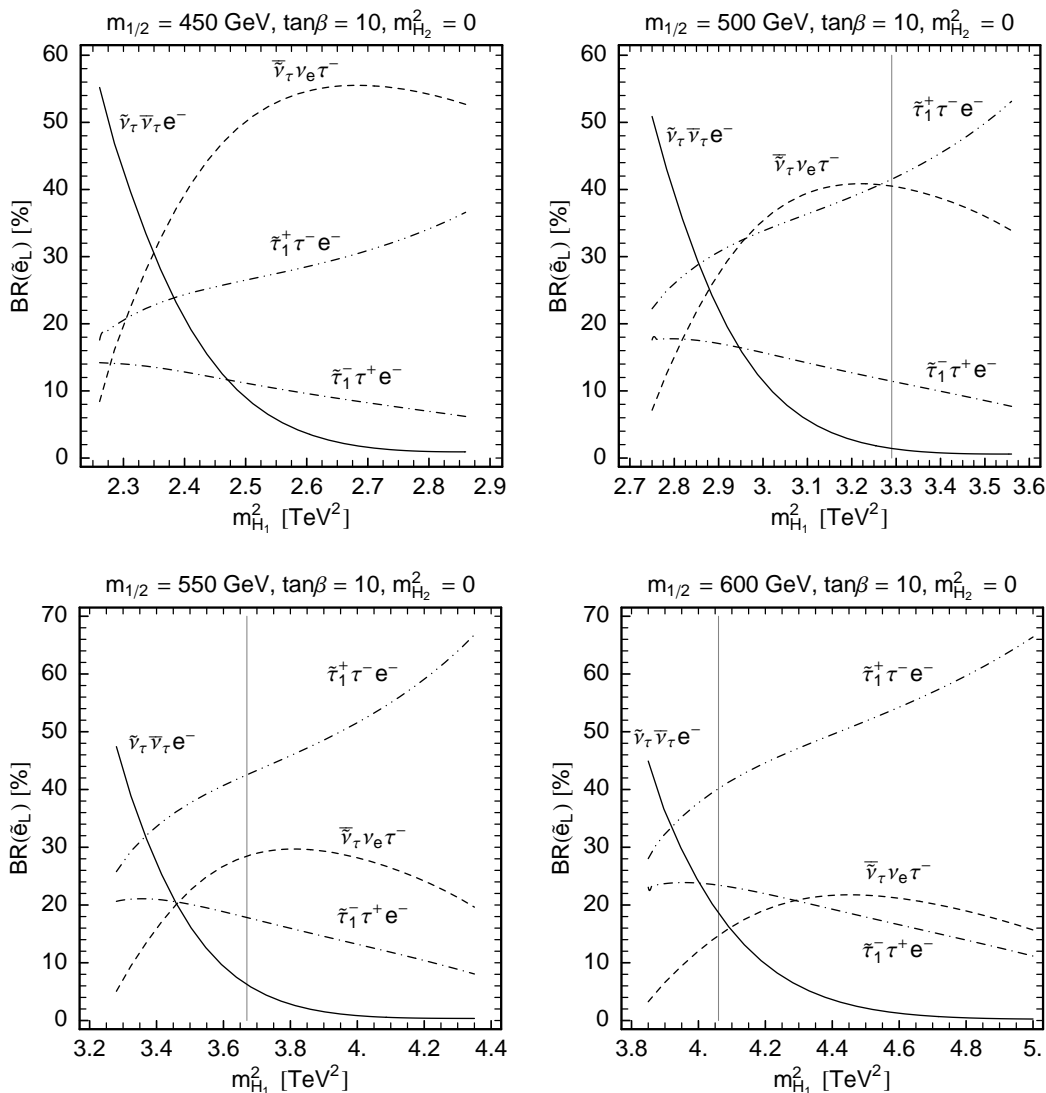


Figure 8: Branching ratios of \tilde{e}_L three-body decays in % as function of $m_{H_1}^2$, for $m_{H_2}^2 = 0$, $\tan\beta = 10$ and $m_{1/2} = 450, 500, 550, 600$ GeV. Only decay modes with sizable BRs are shown. The thin vertical line separates the $\tilde{\nu}_\tau$ NLSP region (to its left) from the $\tilde{\tau}_1$ NLSP region (to its right). In the plot for $m_{1/2} = 450$ GeV, the NLSP is always the $\tilde{\nu}_\tau$.

relatively large $m_{1/2}$, while the decay into $\tilde{\tau}_1^+ e^- \nu_\tau$ becomes dominant in the $\tilde{\tau}_1$ NLSP region for large enough mass splitting. The total decay widths lie in the range of $10^{-7} - 10^{-6}$ GeV.

The last class, $\tilde{\tau}_1$ decays into a $\tilde{\nu}_\tau$ NLSP (or $\tilde{\nu}_\tau$ decays into a $\tilde{\tau}_1$ NLSP) is characterized by a small $\tilde{\tau}_1 - \tilde{\nu}_\tau$ mass difference of only few GeV. Here, the diagram with W exchange is by far the dominant contribution, and the branching ratios are therefore approximately given by those of the W boson. This is illustrated in the left panel of figure 10 for $\tilde{\tau}_1$ decays at $m_{1/2} = 500$ GeV; other values of $m_{1/2}$ give very similar results. As expected, decays into quarks have about 60–70% branching ratio, and decays into electrons or muons about 20%. The decay into $\tilde{\nu}_\tau \tau^- \tilde{\nu}_\tau$ is, however, suppressed by the small $\Delta m = m_{\tilde{\tau}_1} - m_{\tilde{\nu}_\tau}$. One

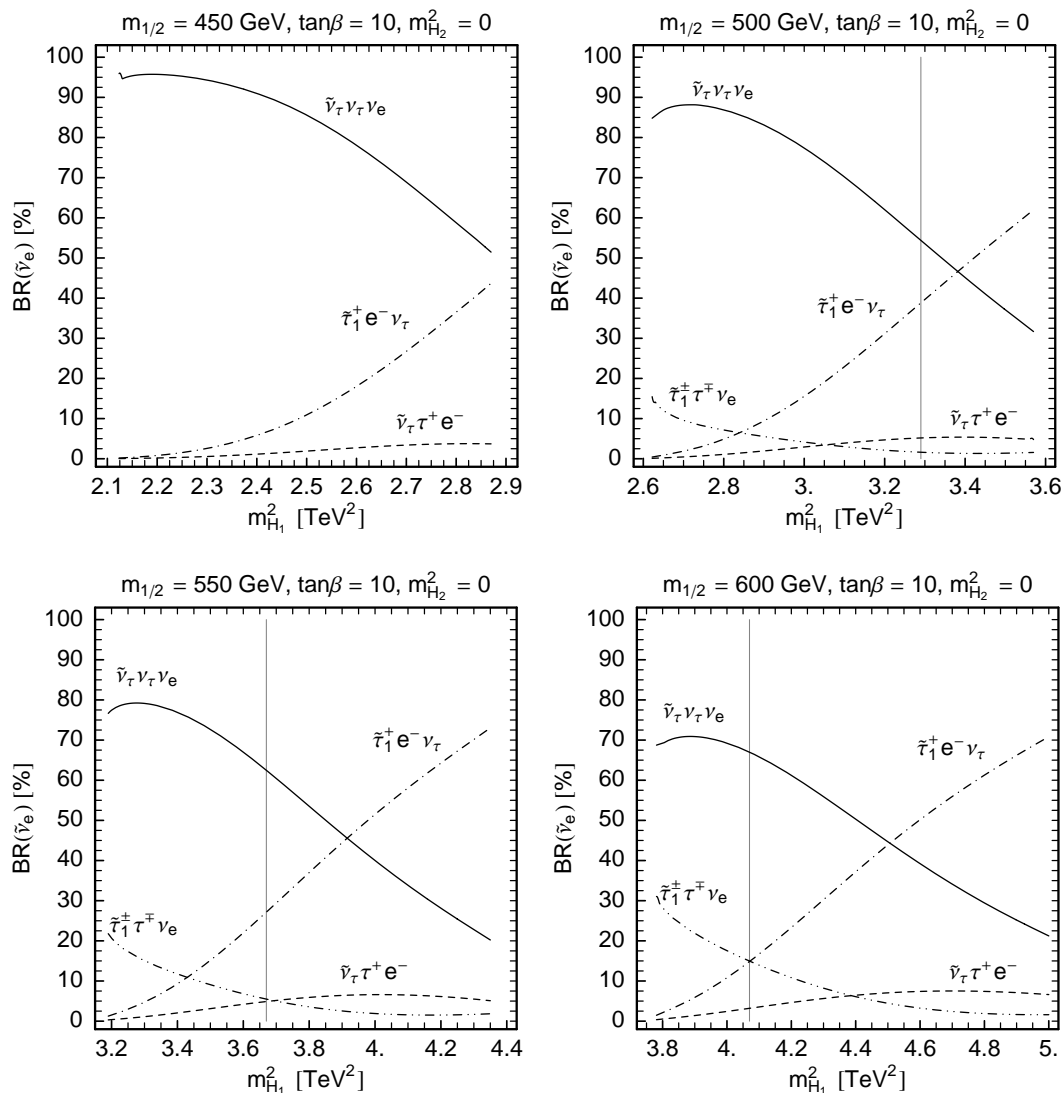


Figure 9: Branching ratios of $\tilde{\nu}_e$ three-body decays in % as function of $m_{H_1}^2$, analogous to figure 8.

can actually see in figure 10 that it goes to zero for $\Delta m < m_\tau$. The total decay width of the $\tilde{\tau}_1$ is about 10^{-8} GeV for $\Delta m = 5\text{--}7$ GeV and about 10^{-11} GeV for $\Delta m \simeq m_\tau$. A displaced vertex only occurs for almost degenerate $\tilde{\tau}_1$ and $\tilde{\nu}_\tau$ ($\Delta m \sim 1$ GeV or smaller). Analogous arguments hold for $\tilde{\nu}_\tau$ decays into a $\tilde{\tau}_1$ NLSP, as can be seen in the right panel of figure 10 for $m_{1/2} = 600$ GeV.

For completeness, we show in figure 11 also the branching ratios for $\tilde{\chi}_1^0$ decays in the parameter range in which the three-body slepton decays are important. The figure is for $m_{1/2} = 500$ GeV; different values of $m_{1/2}$ give similar results. As can be seen, decays into $\tilde{\nu}_\tau \nu_\tau$ dominate. Since the $\tilde{\nu}_\tau$ is the NLSP over most of the region shown, this mode is basically invisible. Comparing with figure 9, also the decays into $\tilde{\nu}_l \nu_l$ are mostly invisible. Visible $\tilde{\chi}_1^0$ signatures result, however, from decays into charged sleptons with about 30–40% branching ratio.

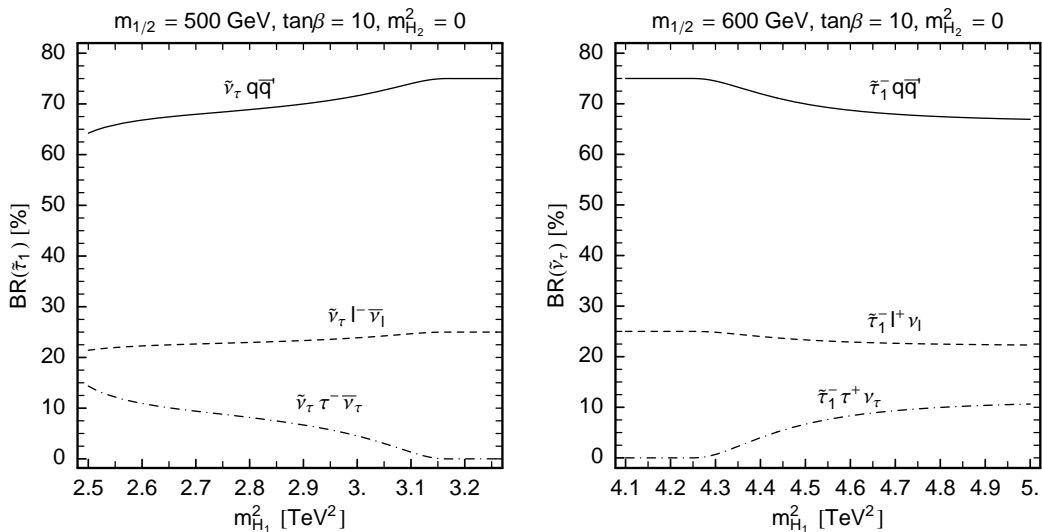


Figure 10: Branching ratios in % for $\tilde{\tau}_1$ decays into a $\tilde{\nu}_\tau$ NLSP (left) and for $\tilde{\nu}_\tau$ decays into a $\tilde{\tau}_1$ NLSP (right).

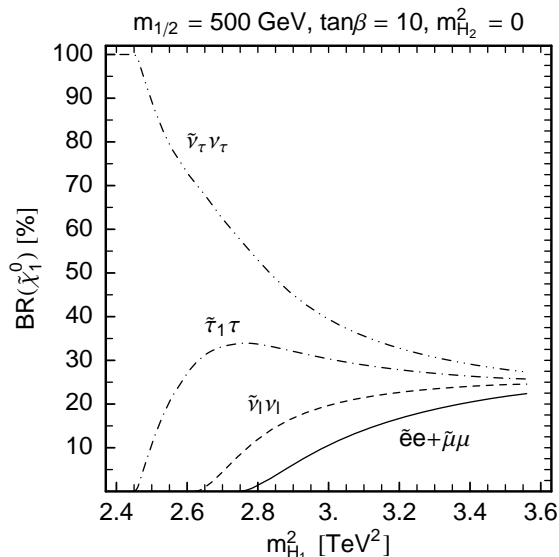


Figure 11: Branching ratios of $\tilde{\chi}_1^0$ decays into sleptons (in %) as function of $m_{H_1}^2$ for $m_{1/2} = 500 \text{ GeV}$.

4. Conclusions

SUSY models with a gravitino LSP and slepton NLSP can have a quite peculiar collider phenomenology. This concerns not only NLSP-to-LSP decays leading to a displaced vertex or happening outside the detector. Also other sleptons besides the NLSP can be lighter than the lightest neutralino, in which case they decay through three-body modes into lighter sleptons, typically the NLSP. So far this had been considered only for right-chiral sleptons in the context of gauge mediation, i.e. three-body decays of \tilde{e}_R and $\tilde{\mu}_R$ into a $\tilde{\tau}_1 \sim \tilde{\tau}_R$ NLSP [19, 20].

In this paper, we discussed an alternative possibility, namely that non-universal Higgs masses cause $\tilde{\ell}_L$ and $\tilde{\nu}_\ell$ to be lighter than $\tilde{\ell}_R$ and $\tilde{\chi}_1^0$. To this aim we used a model of gaugino mediation, which has no-scale boundary conditions for the sfermion mass parameters and trilinear couplings, while $m_{H_{1,2}}^2 \neq 0$. In this model, one can naturally have a gravitino LSP with a mass of $\mathcal{O}(\text{GeV})$, and a $\tilde{\tau}_1 \sim \tilde{\tau}_L$ or $\tilde{\nu}_\tau$ NLSP. Moreover, also \tilde{e}_L , $\tilde{\mu}_L$, and $\tilde{\nu}_{e,\mu}$ can be lighter than the $\tilde{\chi}_1^0$.

We hence computed all slepton three-body decays into other sleptons and implemented them in SDECAY. Here we presented the formulas for $\tilde{\ell}_L$ and $\tilde{\nu}_\ell$ decays and performed a numerical analysis of the branching ratios. We showed that these three-body decays can considerably add to the complexity of SUSY cascade decays; for instance, production and decays of \tilde{e}_L , $\tilde{\mu}_L$ and $\tilde{\nu}_{e,\mu}$ typically lead to complicated mixed-flavour final states. In contrast to the above-mentioned decays of right-chiral sleptons, here decays into sneutrinos are always important even if the NLSP is a $\tilde{\tau}_1$. The decays of $\tilde{\tau}_1$ into $\tilde{\nu}_\tau$ (or vice-versa) can be very well approximated by virtual W exchange. Since the $\tilde{\tau}_1$ - $\tilde{\nu}_\tau$ mass difference is always small, the decay products tend to be soft. A dedicated experimental simulation to assess the potential of future colliders for such a case would be necessary. Last but not least, in the scenario discussed here, the $\tilde{\chi}_1^0$ has visible decays into $\tilde{\ell}^\pm \ell^\mp$ with about 30–40% branching ratio; in the case of $m_{\tilde{\ell}_L} > m_{\tilde{\chi}_1^0} > m_{\tilde{\ell}_R}$, this would be 100%.

Acknowledgments

We are grateful to L. Covi and A. Pukhov for helpful discussions. D.T.N. thanks the CERN Theory Division for hospitality, and UNESCO for financial support. S.K. was supported in part by an APART grant of the Austrian Academy of Sciences.

References

- [1] ATLAS collaboration, *ATLAS detector and physics performance. Technical design report. Vol. 2*, ATLAS-TDR-15 [CERN-LHCC-99-15].
- [2] CMS collaboration, G.L. Bayatian et al., *CMS technical design report, volume II: physics performance*, *J. Phys. G* **34** (2007) 995.
- [3] I. Hinchliffe, F.E. Paige, M.D. Shapiro, J. Soderqvist and W. Yao, *Precision SUSY measurements at LHC*, *Phys. Rev. D* **55** (1997) 5520 [hep-ph/9610544].
- [4] ATLAS and CMS collaborations, J.G. Branson, D. Denegri, I. Hinchliffe, F. Gianotti, F.E. Paige and P. Sphicas, *High transverse momentum physics at the Large Hadron Collider: the ATLAS and CMS collaborations*, *Eur. Phys. J. Direct.* **C 4** (2002) N1.
- [5] B.C. Allanach et al., *SUSY parameter analysis at TeV and Planck scales*, *Nucl. Phys.* **135** (Proc. Suppl.) (2004) 107 [hep-ph/0407067].
- [6] P. Bechtle, K. Desch, W. Porod and P. Wienemann, *Determination of MSSM parameters from LHC and ILC observables in a global fit*, *Eur. Phys. J. C* **46** (2006) 533 [hep-ph/0511006].
- [7] G.L. Kane, P. Kumar, D.E. Morrissey and M. Toharia, *Connecting (supersymmetry) LHC measurements with high scale theories*, *Phys. Rev. D* **75** (2007) 115018 [hep-ph/0612287].

- [8] M. Rauch, R. Lafaye, T. Plehn and D. Zerwas, *SFitter: reconstructing the MSSM Lagrangian from LHC data*, [arXiv:0710.2822](https://arxiv.org/abs/0710.2822).
- [9] LHC/LC STUDY GROUP collaboration, G. Weiglein et al., *Physics interplay of the LHC and the ILC*, *Phys. Rept.* **426** (2006) 47 [[hep-ph/0410364](https://arxiv.org/abs/hep-ph/0410364)].
- [10] CLIC PHYSICS WORKING GROUP collaboration, E. Accomando et al., *Physics at the CLIC multi-TeV linear collider*, [hep-ph/0412251](https://arxiv.org/abs/hep-ph/0412251).
- [11] P. Nath and R. Arnowitt, *Non-universal soft SUSY breaking and dark matter*, *Phys. Rev. D* **56** (1997) 2820 [[hep-ph/9701301](https://arxiv.org/abs/hep-ph/9701301)].
- [12] J.R. Ellis, T. Falk, K.A. Olive and Y. Santoso, *Exploration of the MSSM with non-universal Higgs masses*, *Nucl. Phys. B* **652** (2003) 259 [[hep-ph/0210205](https://arxiv.org/abs/hep-ph/0210205)].
- [13] H. Baer, A. Mustafayev, S. Profumo, A. Belyaev and X. Tata, *Direct, indirect and collider detection of neutralino dark matter in SUSY models with non-universal Higgs masses*, *JHEP* **07** (2005) 065 [[hep-ph/0504001](https://arxiv.org/abs/hep-ph/0504001)].
- [14] W. Buchmüller, J. Kersten and K. Schmidt-Hoberg, *Squarks and sleptons between branes and bulk*, *JHEP* **02** (2006) 069 [[hep-ph/0512152](https://arxiv.org/abs/hep-ph/0512152)].
- [15] J.L. Evans, D.E. Morrissey and J.D. Wells, *Higgs boson exempt no-scale supersymmetry and its collider and cosmology implications*, *Phys. Rev. D* **75** (2007) 055017 [[hep-ph/0611185](https://arxiv.org/abs/hep-ph/0611185)].
- [16] W. Buchmüller, L. Covi, J. Kersten and K. Schmidt-Hoberg, *Dark matter from gaugino mediation*, *JCAP* **11** (2006) 007 [[hep-ph/0609142](https://arxiv.org/abs/hep-ph/0609142)].
- [17] L. Covi and S. Kraml, *Collider signatures of gravitino dark matter with a sneutrino NLSP*, *JHEP* **08** (2007) 015 [[hep-ph/0703130](https://arxiv.org/abs/hep-ph/0703130)].
- [18] M. Muhlleitner, A. Djouadi and Y. Mambrini, *SDECAY: a Fortran code for the decays of the supersymmetric particles in the MSSM*, *Comput. Phys. Commun.* **168** (2005) 46 [[hep-ph/0311167](https://arxiv.org/abs/hep-ph/0311167)].
- [19] S. Ambrosanio, G.D. Kribs and S.P. Martin, *Three-body decays of selectrons and smuons in low-energy supersymmetry breaking models*, *Nucl. Phys. B* **516** (1998) 55 [[hep-ph/9710217](https://arxiv.org/abs/hep-ph/9710217)].
- [20] C.-L. Chou and C.-H. Chou, *Tau polarizations in the three-body slepton decays with stau as the NLSP*, *Phys. Rev. D* **64** (2001) 075008 [[hep-ph/0103116](https://arxiv.org/abs/hep-ph/0103116)].
- [21] G. Bélanger, F. Boudjema, S. Kraml, A. Pukhov and A. Semenov, *Relic density of neutralino dark matter in the MSSM with CP-violation*, *Phys. Rev. D* **73** (2006) 115007 [[hep-ph/0604150](https://arxiv.org/abs/hep-ph/0604150)].
- [22] P. Skands et al., *SUSY Les Houches accord: interfacing SUSY spectrum calculators, decay packages and event generators*, *JHEP* **07** (2004) 036 [[hep-ph/0311123](https://arxiv.org/abs/hep-ph/0311123)].
- [23] A. Djouadi, J. Kalinowski and M. Spira, *HDECAY: a program for Higgs boson decays in the standard model and its supersymmetric extension*, *Comput. Phys. Commun.* **108** (1998) 56 [[hep-ph/9704448](https://arxiv.org/abs/hep-ph/9704448)].
- [24] A. Djouadi, M.M. Muhlleitner and M. Spira, *Decays of supersymmetric particles: the program SUSY-HIT (SUspect-SdecaY-Hdecay-InTerface)*, *Acta Phys. Polon.* **B38** (2007) 635 [[hep-ph/0609292](https://arxiv.org/abs/hep-ph/0609292)]; see also <http://lappweb.in2p3.fr/~muehlleitner/SUSY-HIT/>.
- [25] A. Pukhov, *CalcHEP 3.2: MSSM, structure functions, event generation, batches and generation of matrix elements for other packages*, [hep-ph/0412191](https://arxiv.org/abs/hep-ph/0412191).

- [26] D.E. Kaplan, G.D. Kribs and M. Schmaltz, *Supersymmetry breaking through transparent extra dimensions*, *Phys. Rev. D* **62** (2000) 035010 [[hep-ph/9911293](#)].
- [27] Z. Chacko, M.A. Luty, A.E. Nelson and E. Ponton, *Gaugino mediated supersymmetry breaking*, *JHEP* **01** (2000) 003 [[hep-ph/9911323](#)].
- [28] B.C. Allanach, *SOFTSUSY: a C++ program for calculating supersymmetric spectra*, *Comput. Phys. Commun.* **143** (2002) 305 [[hep-ph/0104145](#)].
- [29] W. Buchmüller, K. Hamaguchi and J. Kersten, *The gravitino in gaugino mediation*, *Phys. Lett. B* **632** (2006) 366 [[hep-ph/0506105](#)].